Electronic Supplementary Information

# Bis(alkyl) Scandium and Yttrium Complexes Coordinated by an Amidopyridinate Ligand: Synthesis, Characterization and Catalytic Performance in Isoprene Polymerization, Hydroelementation and Carbon Dioxide Hydrosilylation

G. A. Gurina,[a] A. A. Kissel,[a,b] D. M. Lyubov,[a] L. Luconi,[c] A. Rossin,[c] G. Tuci,[c] A. V. Cherkasov,[a] K. A. Lyssenko,[a] A. S. Shavyrin,[a] A. M. Ob'edkov,[a] G. Giambastiani*[c, d, e] and A. A. Trifonov *[a, b]

[a.] *Institute of Organometallic Chemistry of Russian Academy of Sciences, Tropinina str. 49, GSP–445, 603950 Nizhny Novgorod, Russia*
[b.] *Institute of Organoelement Compounds of Russian Academy of Sciences, Vavilova str. 28, 119334 Moscow, Russia*
[c.] *Institute of Chemistry of OrganoMetallic Compounds, ICCOM-CNR and Consorzio INSTM, Via Madonna del Piano, 10 – 50019, Sesto F.no, Florence, Italy*
[d.] *Institute of Chemistry and Processes for Energy, Environment and Health (ICPEES), UMR 7515 CNRS- University of Strasbourg (UdS), 25, rue Becquerel, 67087 Strasbourg Cedex 02, France*
[e.] *Kazan Federal University, 420008 Kazan, Russian Federation*

Contents:

# Electronic Supplementary Information



**Table S1.** Crystal data and structure refinement details for $\mathbf{1_{Sc}}$, $\mathbf{1_Y}$ and $\mathbf{1_Y^{THF}}$.

| | $\mathbf{1_{Sc}}$ | $\mathbf{1_Y}$ | $\mathbf{1_Y^{THF}}$ |
|---|---|---|---|
| Formula | $C_{36}H_{55}N_4OScSi_2$, $C_7H_8$ | $C_{36}H_{55}N_4OSi_2Y$, $1½C_7H_8$ | $C_{40}H_{63}N_4O_2Si_2Y$, $½C_6H_{14}$ |
| M | 753.11 | 843.13 | 820.12 |
| *T*, K | 120 | 100 | 120 |
| Crystal system | Monoclinic | Monoclinic | Triclinic |
| Space group | *P2$_1$/c* | *C2/c* | *P-1* |
| *a*, Å | 19.191(2) | 22.2860(10) | 11.6694(6) |
| *b*, Å | 16.3197(18) | 15.6506(7) | 13.2058(7) |
| *c*, Å | 14.8442(16) | 26.8173(12) | 17.2330(9) |
| *α*, deg | 90 | 90 | 112.2250(10) |
| *β*, deg | 108.715(3) | 90.9180(10) | 104.7190(10) |
| *γ*, deg | 90 | 90 | 91.7040(10) |
| *V*, Å$^3$ | 4403.3(8) | 9352.4(7) | 2354.1(2) |
| *Z* | 4 | 8 | 2 |
| $d_{calc}$, g/cm$^3$ | 1.136 | 1.198 | 1.157 |
| *μ*, mm$^{-1}$ | 0.257 | 1.335 | 1.325 |
| $F_{000}$ | 1624 | 3592 | 878 |
| Crystal dimensions, mm | 0.35×0.25×0.18 | 0.34×0.18×0.10 | 0.31×0.12×0.07 |
| *θ* range for data collection, deg | 1.12–26.02 | 1.77–29.13 | 1.68–30.03 |

| | | | |
|---|---|---|---|
| *HKL* indices | $-23 \le h \le 23$<br>$-20 \le k \le 20$<br>$-18 \le l \le 18$ | $-30 \le h \le 30$<br>$-21 \le k \le 21$<br>$-36 \le l \le 36$ | $-16 \le h \le 16$<br>$-18 \le k \le 18$<br>$-24 \le l \le 24$ |
| Reflns. collected | 56077 | 50513 | 31664 |
| Reflns. unique | 8683 | 12580 | 13779 |
| $R_{int}$ | 0.1155 | 0.0822 | 0.0508 |
| Data / restraints / parameters | 56077 / 99 / 513 | 12580 / 291 / 552 | 13779 / 42 / 500 |
| $S(F^2)$ | 1.010 | 1.056 | 1.007 |
| $R_1/wR_2$ ($I > 2\sigma(I)$) | 0.0535 / 0.1280 | 0.0590 / 0.1200 | 0.0474 / 0.0981 |
| $R_1/wR_2$ (all data) | 0.0876 / 0.1490 | 0.1029 / 0.1383 | 0.0845 / 0.1101 |
| Largest diff. peak and hole, e/Å$^3$ | 1.12 / –0.45 | 1.10 / –0.58 | 0.97 / –0.63 |

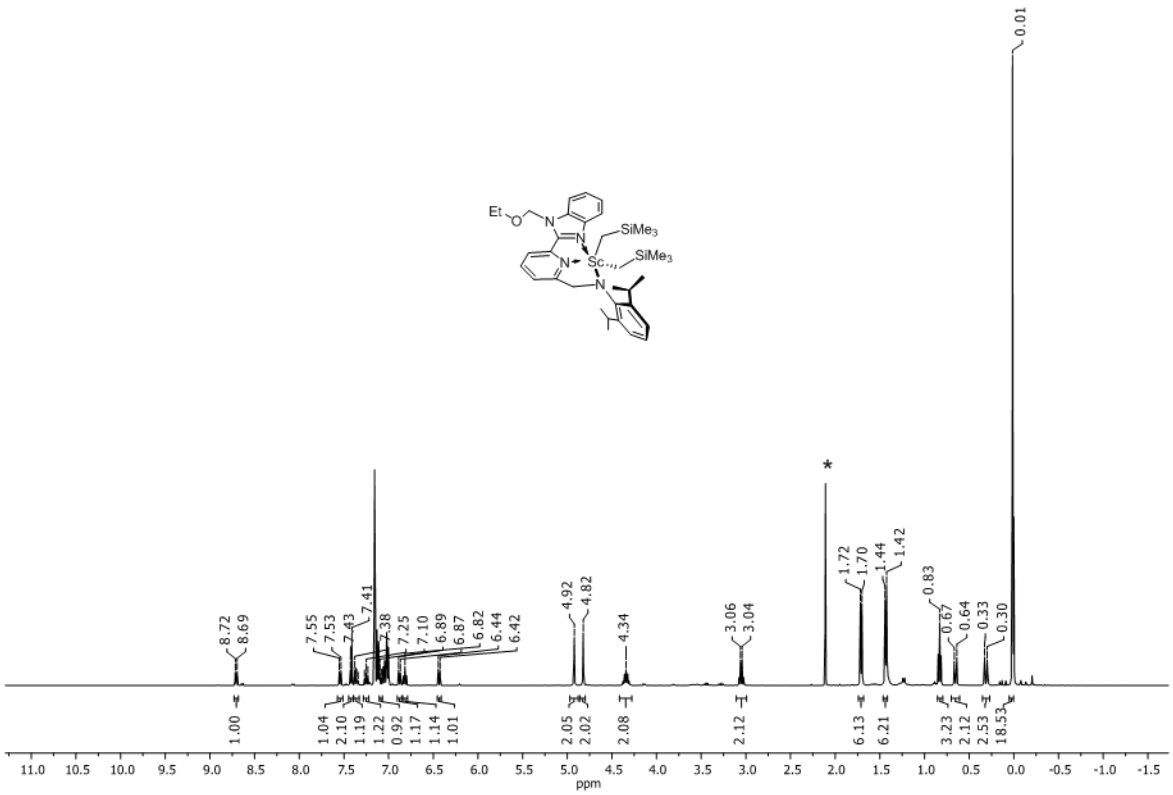


**Fig. S1.** $^1$H NMR spectrum (400 MHz, $C_6D_6$, 293 K) of **1**$_{Sc}$. *signal of toluene solvate.

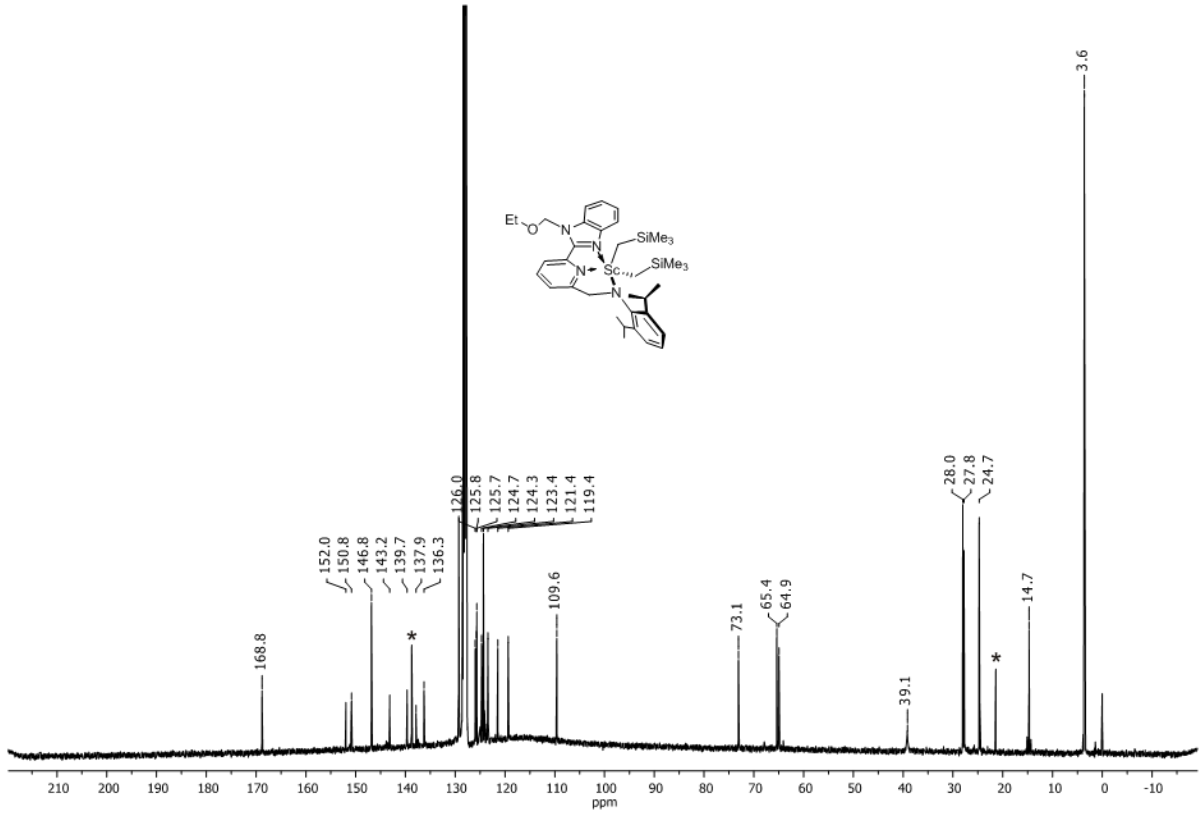


**Fig. S2.** $^{13}C\{^{1}H\}$ NMR spectrum (100 MHz, $C_6D_6$, 293 K) of $\mathbf{1_{Sc}}$. *signal of toluene solvate.

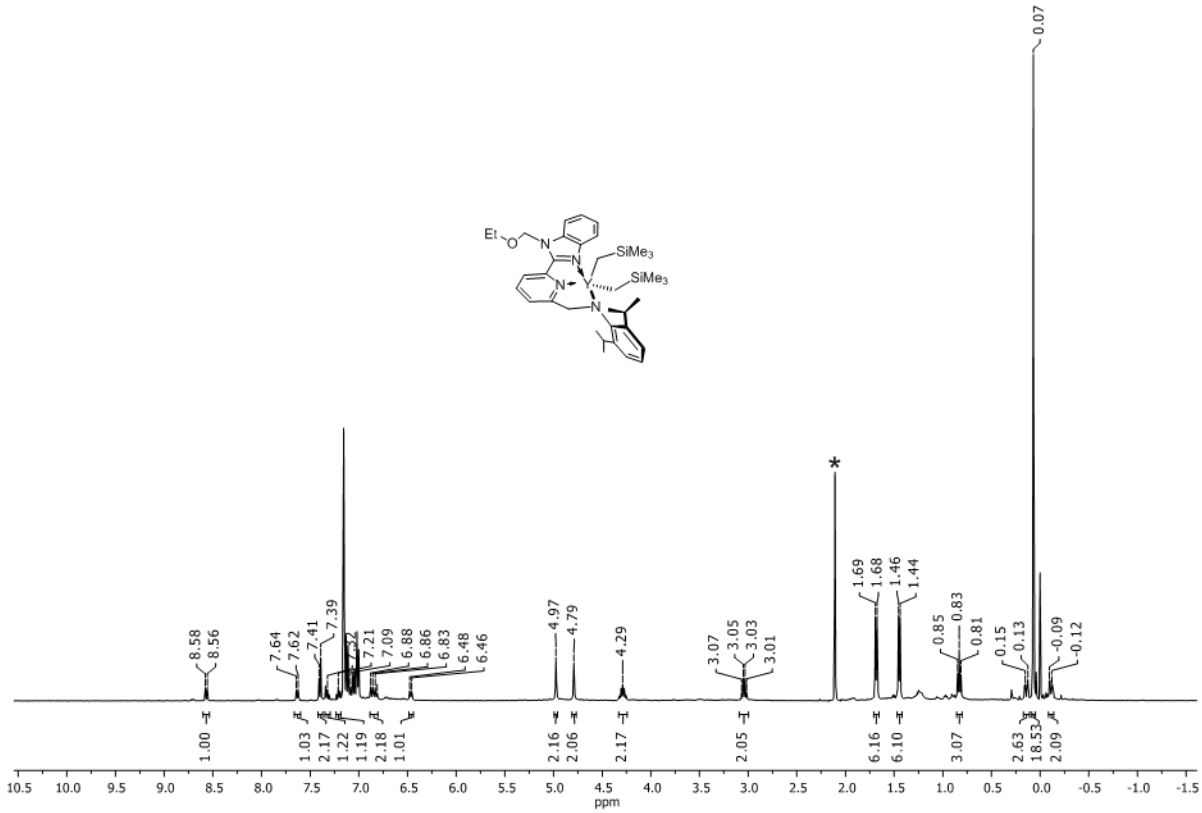


**Fig. S3.** $^{1}H$ NMR spectrum (400 MHz, $C_6D_6$, 293 K) of $\mathbf{1_Y}$. *signal of toluene solvate.

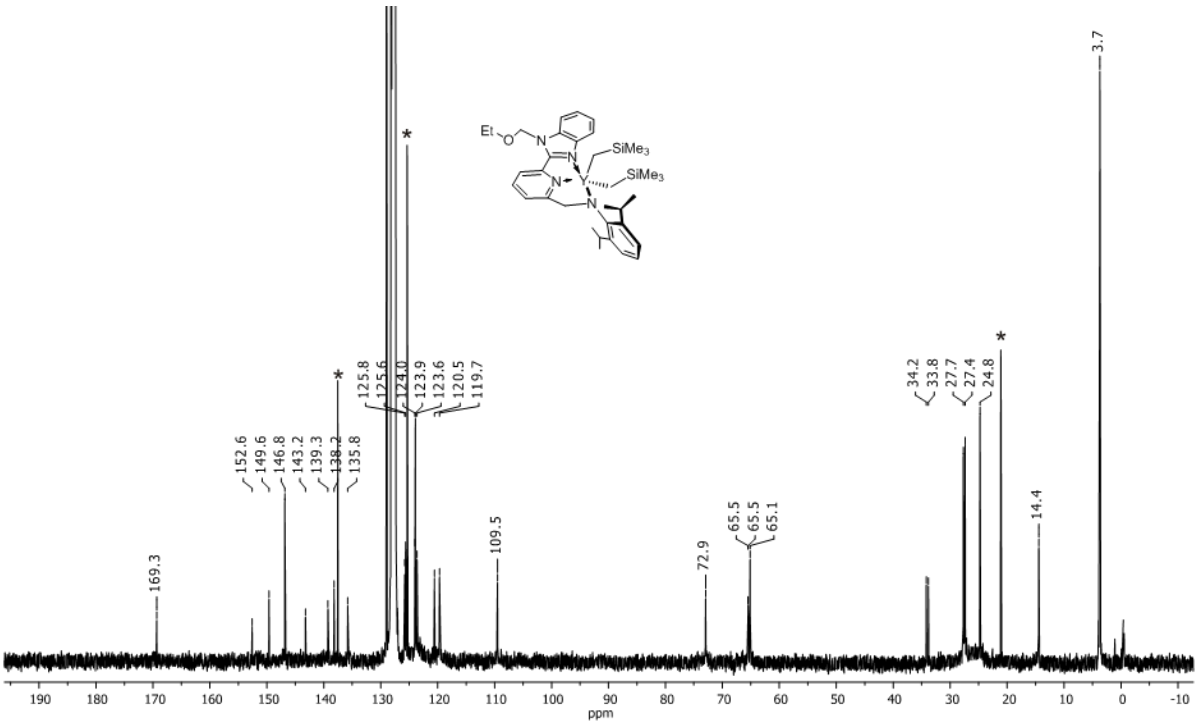


**Fig. S4.** $^{13}C\{^{1}H\}$ NMR spectrum (100 MHz, $C_6D_6$, 293 K) of $\mathbf{1_Y}$. *signal of toluene solvate.

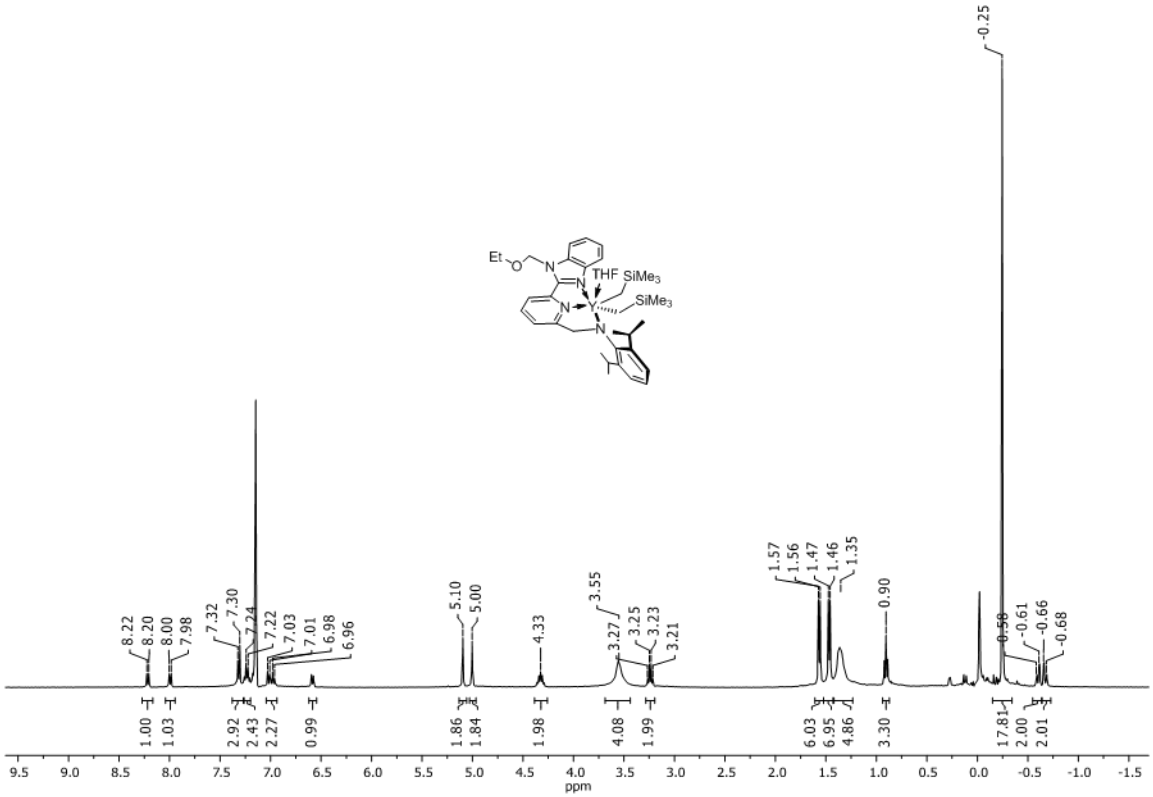


**Fig. S5.** $^{1}H$ NMR spectrum (400 MHz, $C_6D_6$, 293 K) of $\mathbf{1_Y^{THF}}$.

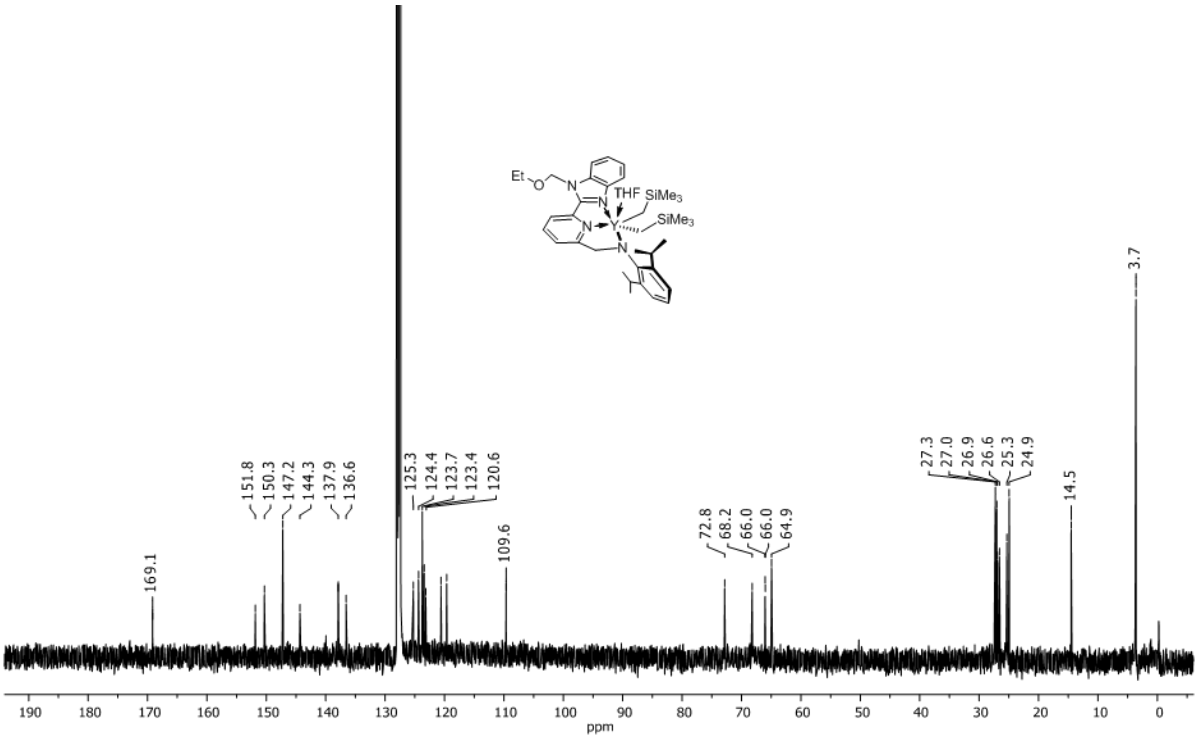


**Fig. S6.** $^{13}C\{^{1}H\}$ NMR spectrum (100 MHz, $C_6D_6$, 293 K) of $\mathbf{1_Y^{THF}}$.

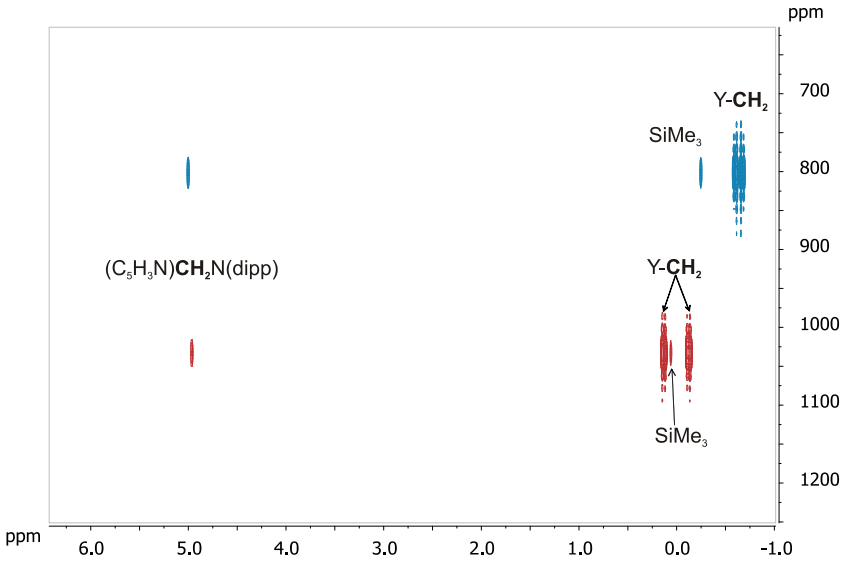


**Fig. S7.** 2D $^{89}Y$-$^{1}H$ *g*-HMQC NMR spectrum (400; 19.6 MHz, $C_6D_6$, 293 K) of $\mathbf{1_Y}$ (red) and $\mathbf{1_Y^{THF}}$ (blue).

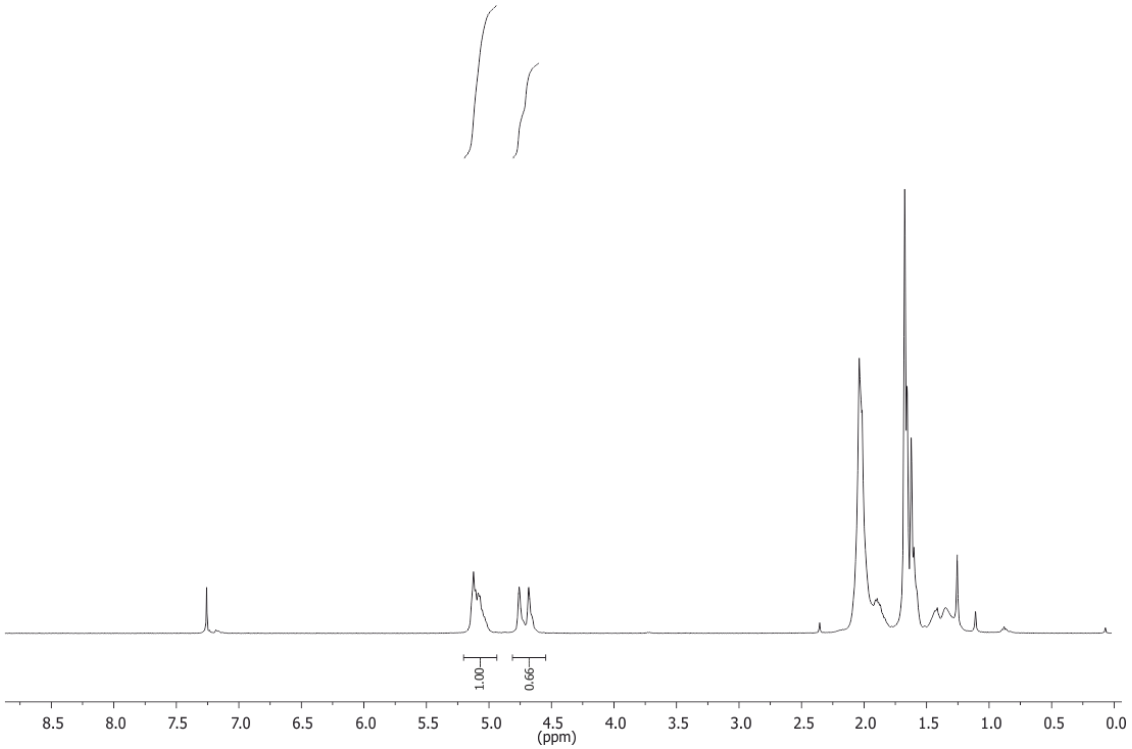


**Fig. S8**. $^{1}H$ NMR spectrum (400 MHz, $CDCl_3$, 293 K) of PIP prepared by catalysis with **1sc**/[$PhNHMe_2$] [$B(C_6F_5)_4$]/Al$^{i}$$Bu_3$ ternary system (from Table 2, entry 5).

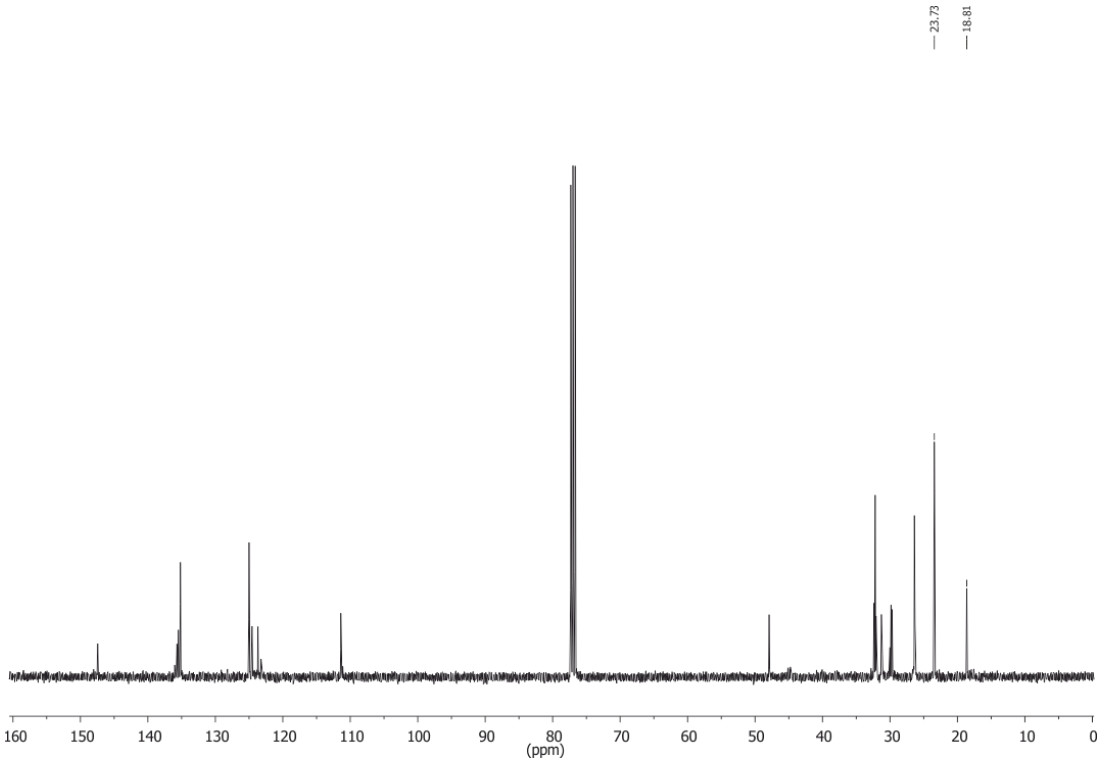


**Fig. S9**. $^{13}C\{^{1}H\}$ NMR spectrum (100 MHz, $CDCl_3$, 293 K) of PIP prepared by catalysis with **1sc**/[$PhNHMe_2$] [$B(C_6F_5)_4$]/Al$^{i}$$Bu_3$ ternary system (from Table 2, entry 5).

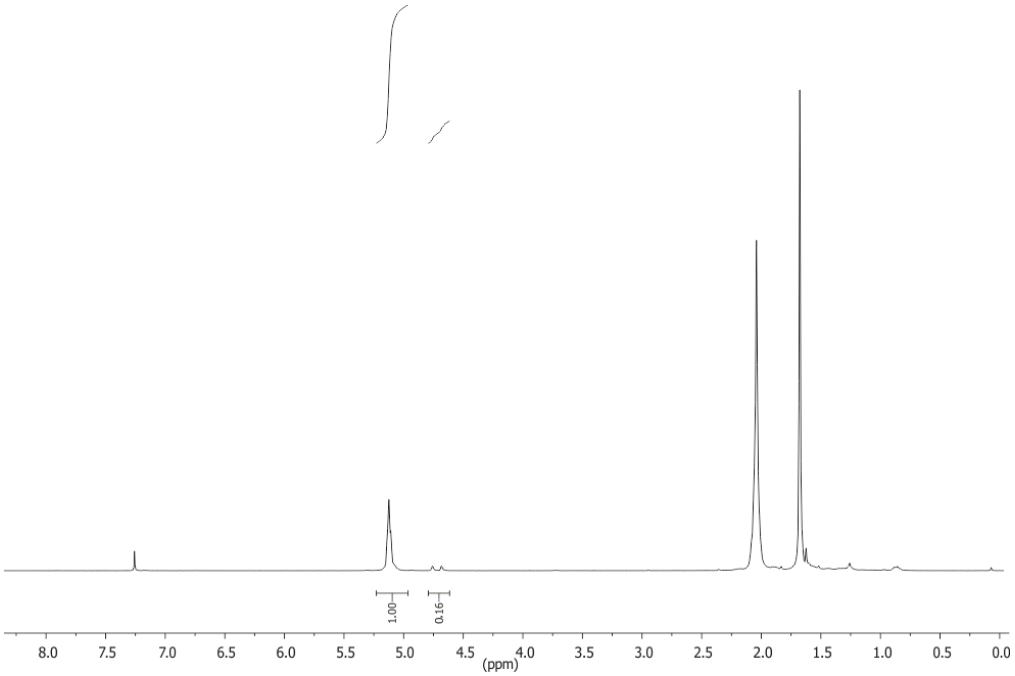


**Fig. S10**. $^{1}$H NMR spectrum (400 MHz, $CDCl_3$, 293 K) of PIP prepared by catalysis with **1Y**/$[Ph_3C][B(C_6F_5)_4]$/Al$^{i}$Bu$_3$ ternary system (from Table 2, entry 9).

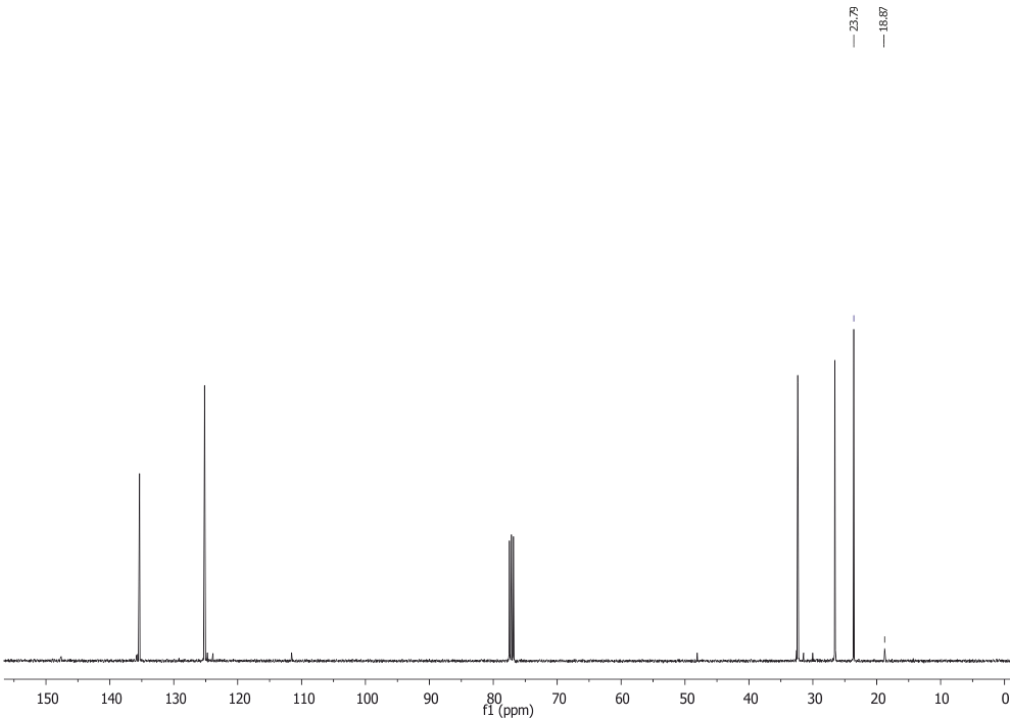


**Fig. S11**. $^{13}C\{^{1}H\}$ NMR spectrum (100 MHz, $CDCl_3$, 293 K) of PIP prepared by catalysis with **1Y**/$[Ph_3C][B(C_6F_5)_4]$/Al$^{i}$Bu$_3$ ternary system (from Table 2, entry 9).

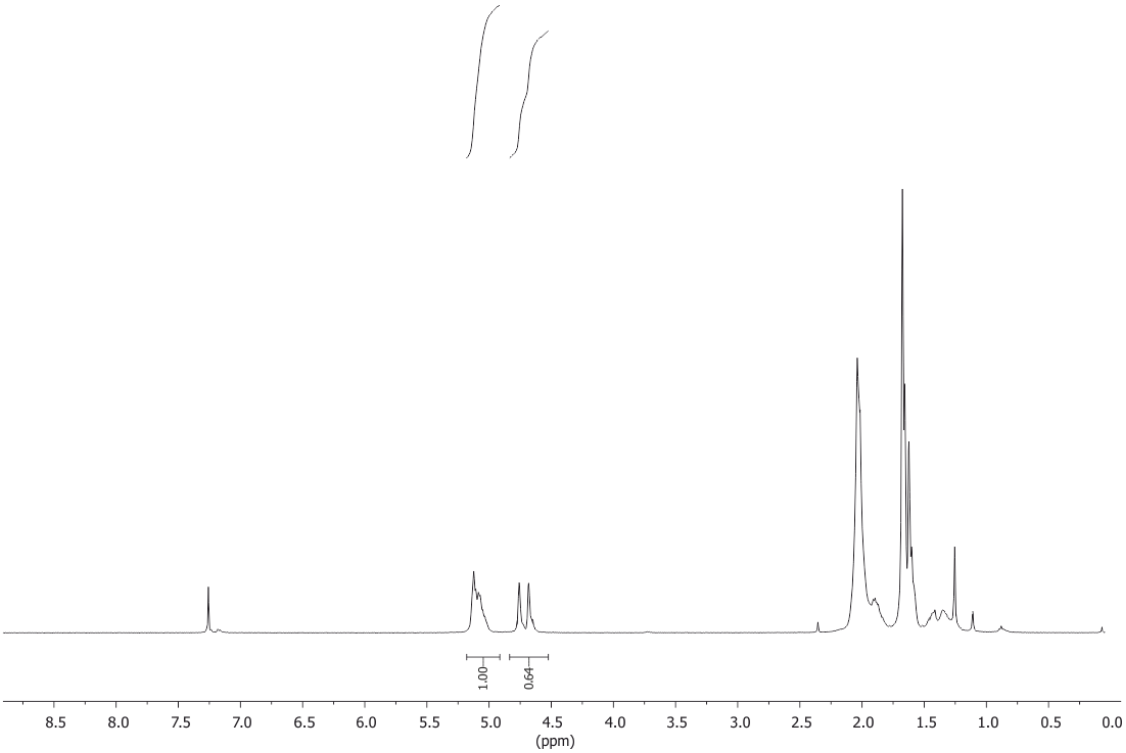


**Fig. S12**. $^{1}$H NMR spectrum (400 MHz, $CDCl_3$, 293 K) of PIP prepared by catalysis with $\mathbf{1_Y^{THF}}$/[$PhNHMe_2$][$B(C_6F_5)_4$]/Al$^{i}$$Bu_3$ ternary system (from Table 2, entry 11).

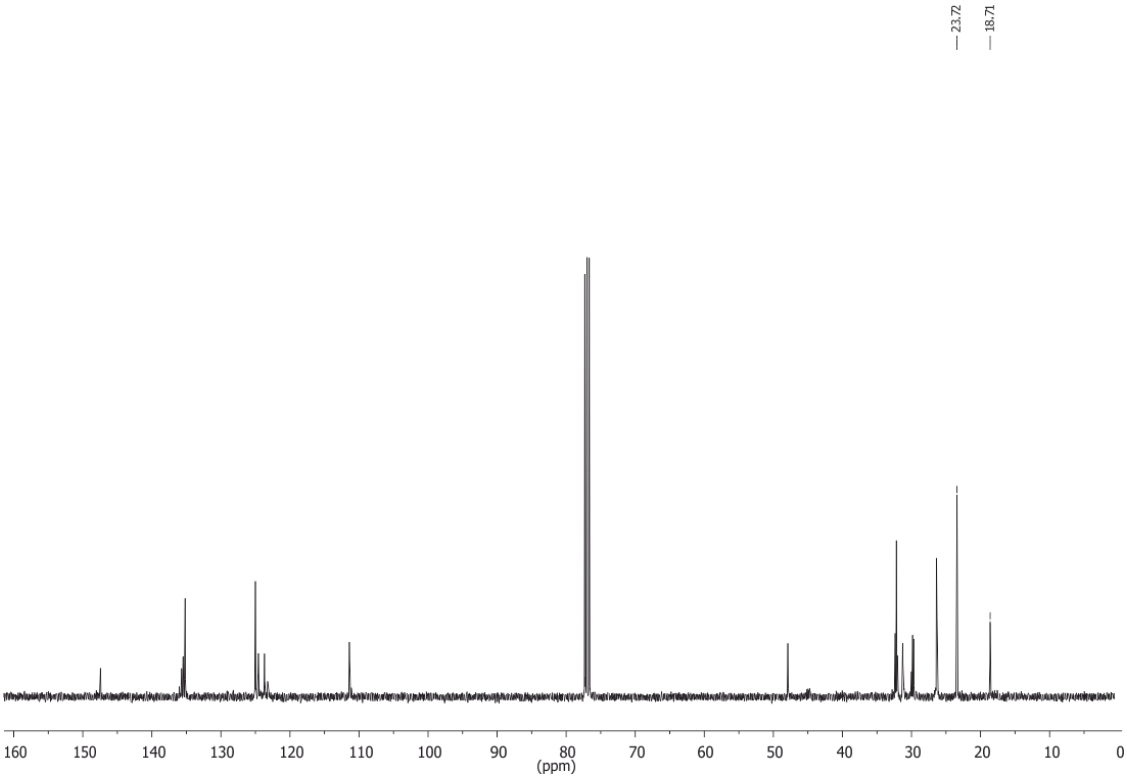


**Fig. S13**. $^{13}C\{^{1}H\}$ NMR spectrum (100 MHz, $CDCl_3$, 293 K) of PIP prepared by catalysis with $\mathbf{1_Y^{THF}}$/[$PhNHMe_2$][$B(C_6F_5)_4$]/Al$^{i}$$Bu_3$ ternary system (from Table 2, entry 11).

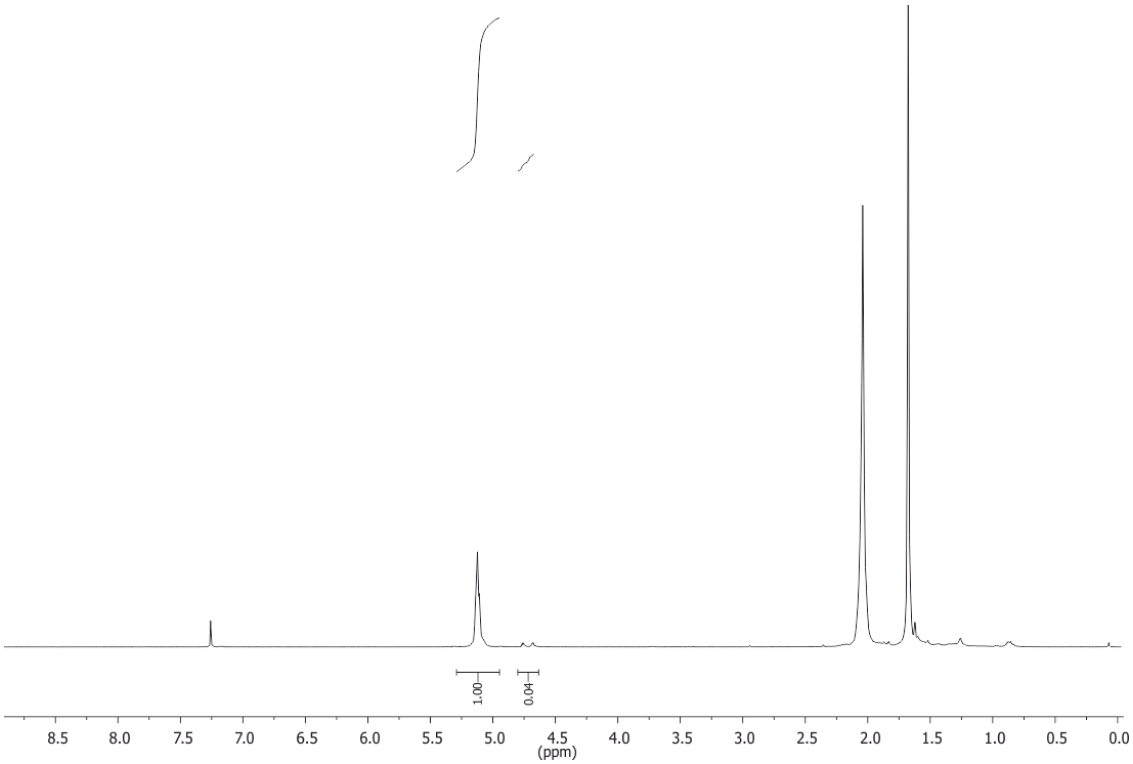


**Fig. S14**. $^{1}$H NMR spectrum (400 MHz, $CDCl_3$, 293 K) of PIP prepared by catalysis with $\mathbf{1_Y}^{\mathbf{THF}}$/$[Ph_3C][B(C_6F_5)_4]$/Al$^{i}$Bu$_3$ ternary system (from Table 2, entry 13).

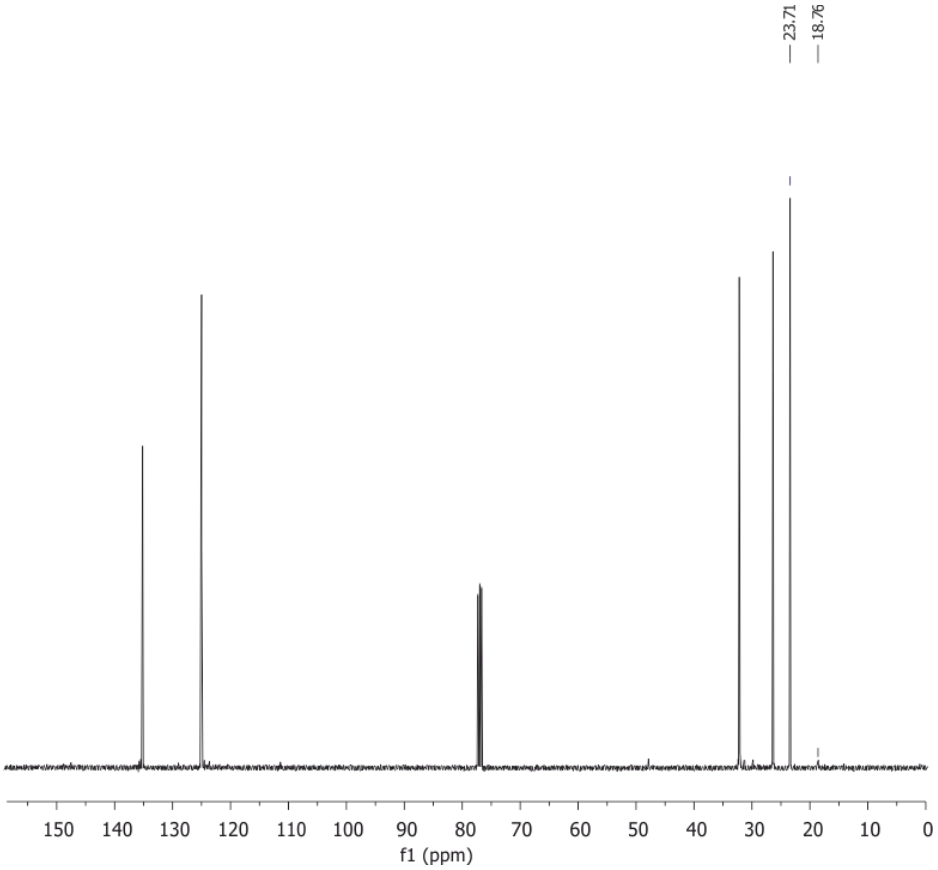


**Fig. S15**. $^{13}$C{$^{1}$H } NMR spectrum (100 MHz, $CDCl_3$, 293 K) of PIP prepared by catalysis with $\mathbf{1_Y}^{\mathbf{THF}}$/$[Ph_3C][B(C_6F_5)_4]$/Al$^{i}$Bu$_3$ ternary system (from Table 2, entry 13).

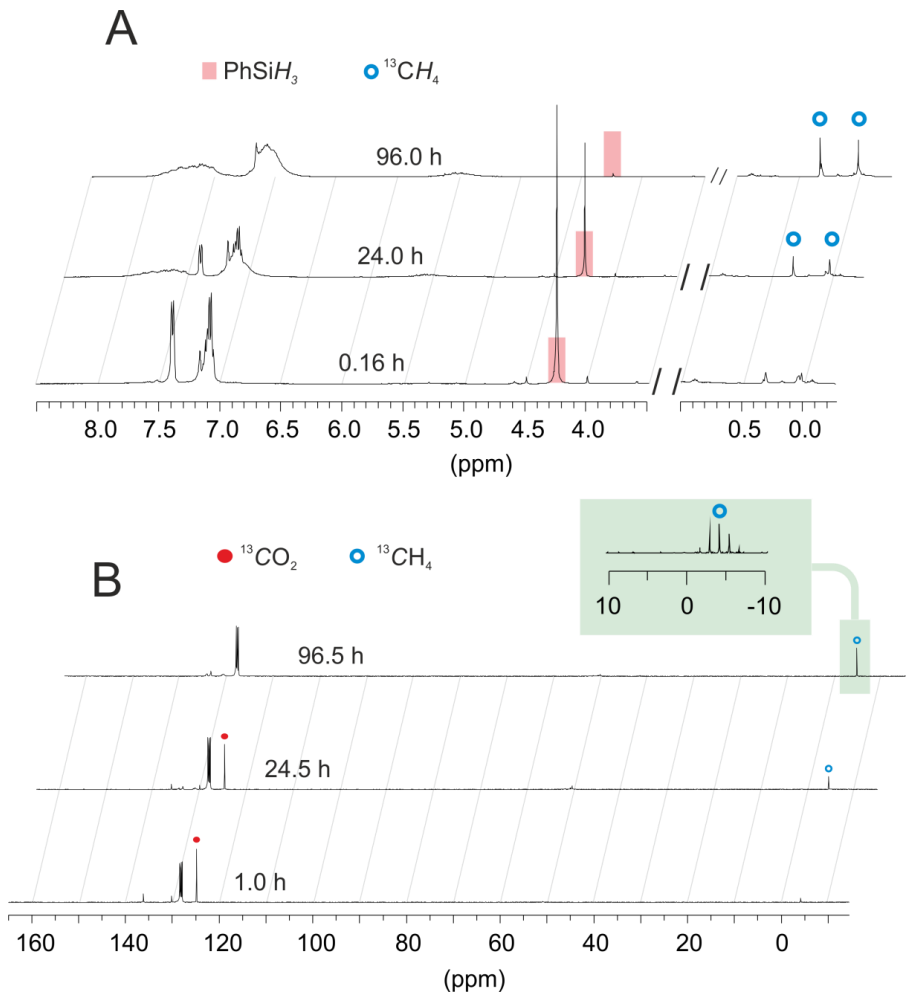


**Fig. S16.** $^{1}H$ and $^{13}C\{^{1}H\}$ NMR spectra (400 MHz, $C_6D_6$, 298 K) recorded at variable time for the $^{13}CO_2$ hydrosilylation reaction, using $PhSiH_3$ as reductant. Conditions: r.t., **1Y*** (1.5 mol % vs. $PhSiH_3$); (Y/B = 1/1.1). green inset $^{13}C$ NMR spectrum